

1 **Version of the attached file:** Non-peer reviewed preprint submitted to EarthArxiv₁

2 **Peer-reviewed status of the attached File:** Non-peer reviewed₂

3 **Citation for the pre-print file:** Shaw, J.B., K.G. Mason, H. Ma, G. McCain (2020), Influences on
4 Discharge Partitioning on a Large River Delta: Case Study of the Mississippi-Atchafalaya Diversion,
5 1916-1950, EarthArxiv: <https://osf.io/w3rxp>

6 **Additional information:** This manuscript is a preprint and has been submitted to Water Resources
7 Research for publication. The manuscript version posted on EarthArxiv is non-peer reviewed and
8 subsequent versions of the manuscript may differ from this version. If the manuscript is accepted for
9 publication, the final typeset version will be available via the "Peer-reviewed Publication DOI" link on the
10 right hand side of this web page. Please feel free to contact any of the authors, we welcome feedback.

11 **Influences on Discharge Partitioning on a Large River Delta: Case Study of the**
12 **Mississippi-Atchafalaya Diversion, 1916-1950**

13 **John B. Shaw¹, Kashauna G. Mason^{1,†}, Hongbo Ma¹, Gordon McCain¹**

14 ¹Department of Geosciences, University of Arkansas, Fayetteville, AR, 72701

15 Corresponding author: John Shaw (shaw84@uark.edu)

16 †Currently at Department of Geology and Geophysics, Texas A&M University, College Station,
17 TX, 77843.

18 **Key Points:**

- 19 • The rapid increase in discharge to the Atchafalaya River between 1932 and 1950 can be
20 explained first by widening and second by dredging.
- 21 • Minor erosion measured in the Mississippi River would have reduced Atchafalaya
22 Discharge, had Atchafalaya Basin remained constant.
- 23 • Lacustrine Deltas in the Atchafalaya Basin did not change partitioning, as they were
24 downstream of a reach with steep water surface slope.
25

26 **Abstract**

27 The modern Mississippi River Delta is plumed by the Mississippi and Atchafalaya rivers,
28 setting water and sediment dispersal pathways for Earth's fifth-largest river. The Atchafalaya
29 River's (AR) partial annexation of discharge from the Mississippi River (MR) in the early 20th
30 century prompted warnings of a rapid river avulsion and the construction of the Old River
31 Control Structure to regulate flow. While this flow annexation is interpreted as a natural process
32 in the avulsion-constructed delta, it was influenced by human activities. Here, we test how
33 several significant changes between 1916 and 1950 influenced partitioning. Simulations show
34 that erosion of the upper AR was the primary cause of discharge increase. Dredging in the lower
35 AR between 1932 and 1950 produced minor increases, but was an important control on shear
36 stress. The lower MR was also slightly erosional during the study period, and therefore hindered
37 the discharge increase slightly. As a prototype system, attribution of discharge partitioning
38 allows for various drivers of change to be quantitatively compared. Given the essential nature of
39 this river junction to society, transportation, and commerce of the United States, improved
40 attribution of discharge increases may lead to future management strategies that are broadly
41 impactful.

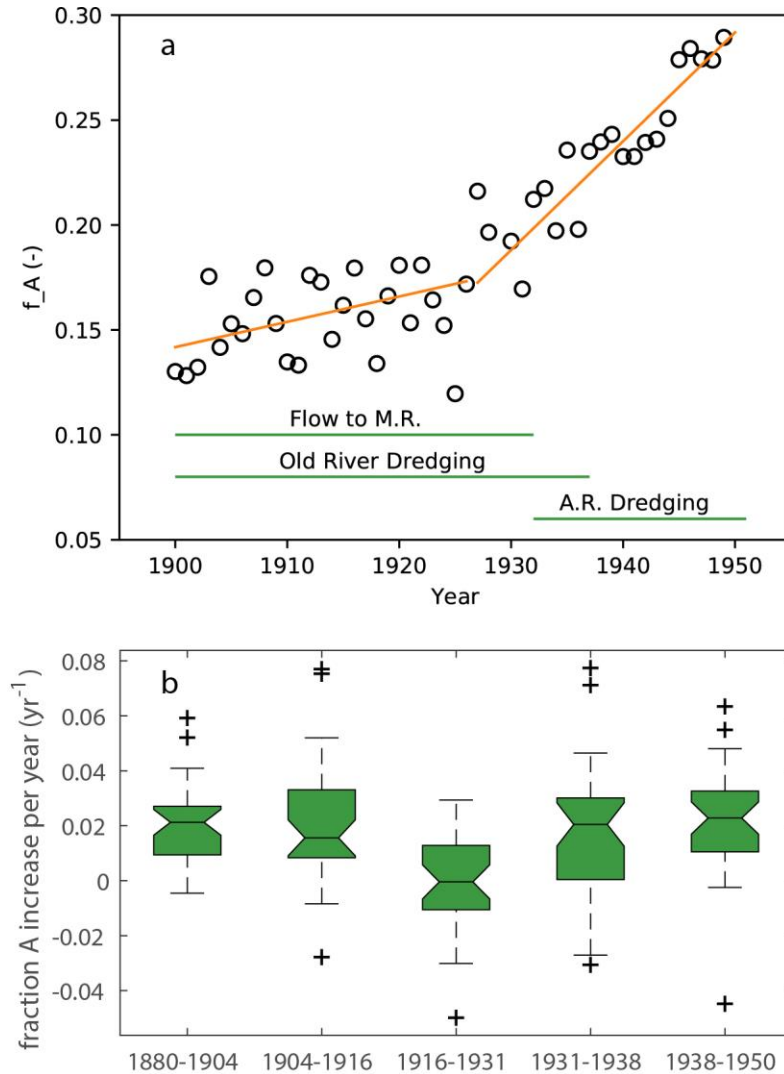
42 **1 Introduction**

43 Many of the world's large river deltas evolve under a combination of natural and human forcings
44 (Ganti et al., 2014; Kleinhans et al., 2011; Vinh et al., 2014; Wilson et al., 2017). However,
45 frameworks for attributing change among several forcings that occur simultaneously remain
46 elusive. The problem is further compounded by the complexity of many river deltas, where
47 forcings interact non-locally through a network of many distributary channels (Bain et al., 2019;
48 Kleinhans et al., 2012). Constraining these interactions is essential for the many large scale
49 management and engineering initiatives that will significantly alter modern deltas to optimize for
50 their sustainable future (Hoitink et al., 2020; Syvitski, 2008; Tessler et al., 2015). Here, we present
51 one such case of complex interaction of many forcings across the channel network of a large river
52 delta.

53 The regulation of water discharge between the Mississippi and Atchafalaya Rivers is one of the
54 most impressive river engineering feats of the twentieth century. The Old River Control Structure
55 (ORCS) ensures that 70% of water discharge travels down the lower Mississippi River, through
56 the cities of Baton Rouge and New Orleans, and the largest port in the western hemisphere (Batker
57 et al., 2014). The remaining 30% of the discharge passes through the structure and down the
58 Atchafalaya River to build significant new delta deposits in Atchafalaya Bay (Roberts et al., 1980;
59 J. B. Shaw et al., 2018). The ORCS was constructed for \$67 million and completed in 1962, but
60 required an additional auxiliary structure costing \$206 million, completed in 1982 (USACE, 2009)
61 for a total cost in 2009 dollars of roughly \$990 million (Kenney et al., 2013).

62 The modern system is the product of natural processes across the geologic time (Blum, 2019;
63 Saucier, 1994) and human activities since the nineteenth century (Kesel, 2003; Mossa, 2013). Over
64 the Holocene, the Mississippi River delta has been dominated by semi-periodic avulsions, or the
65 rapid abandonment of a channel course for a new course through the delta (Blum & Roberts, 2012;
66 Fisk, 1952; Saucier, 1994). Human impacts include dredged meander cutoffs that straightened the
67 Mississippi River's course (1831-1942), and large log jams that were removed from the
68 Atchafalaya River (1839-1855; Mossa, 2013). At Red River Landing, where the Old River (an

69 abandoned meander loop) connects the Mississippi and Atchafalaya rivers, a canal was dredged
 70 intermittently between 1878 and 1937 in order to maintain navigable low-water connection
 71 between the rivers (Fisk, 1952; Mossa, 2013). Between 1900 and 1932, the Atchafalaya River
 72 flowed into the Mississippi River an average of 37 days per year, with the last flow in this direction
 73 in 1945 (Latimer and Schweizer 1951; their Table 36). After the great flood of 1929, significant
 74 levee construction and dredging along the Mississippi and Atchafalaya Rivers influenced
 75 navigability and hydrology of both rivers.



76
 77 **Figure 1.** (a) Time series of the proportion of water entering the Atchafalaya River from the
 78 Mississippi River f_A . Orange lines are linear fits to f_A for the periods 1900-1926 and 1927-1950.
 79 Green bars indicate time periods of potentially important events. A.R. and M.R. signify
 80 Atchafalaya and Mississippi Rivers. (b) Notched box plots (Kafadar, 2014) of increase in bank-
 81 full cross-sectional area per year between USACE hydrographic surveys ($0.02 = 2\%$ average
 82 increase per year) for $n=35$ transects in the 66 km downstream of Red River Landing (compiled
 83 by McCain, 2016). Box shows interquartile range (IQR). Whiskers show one IQR above and below
 84 box. Plusses show outliers. Line is median. Notch is the 95% confidence interval of the median

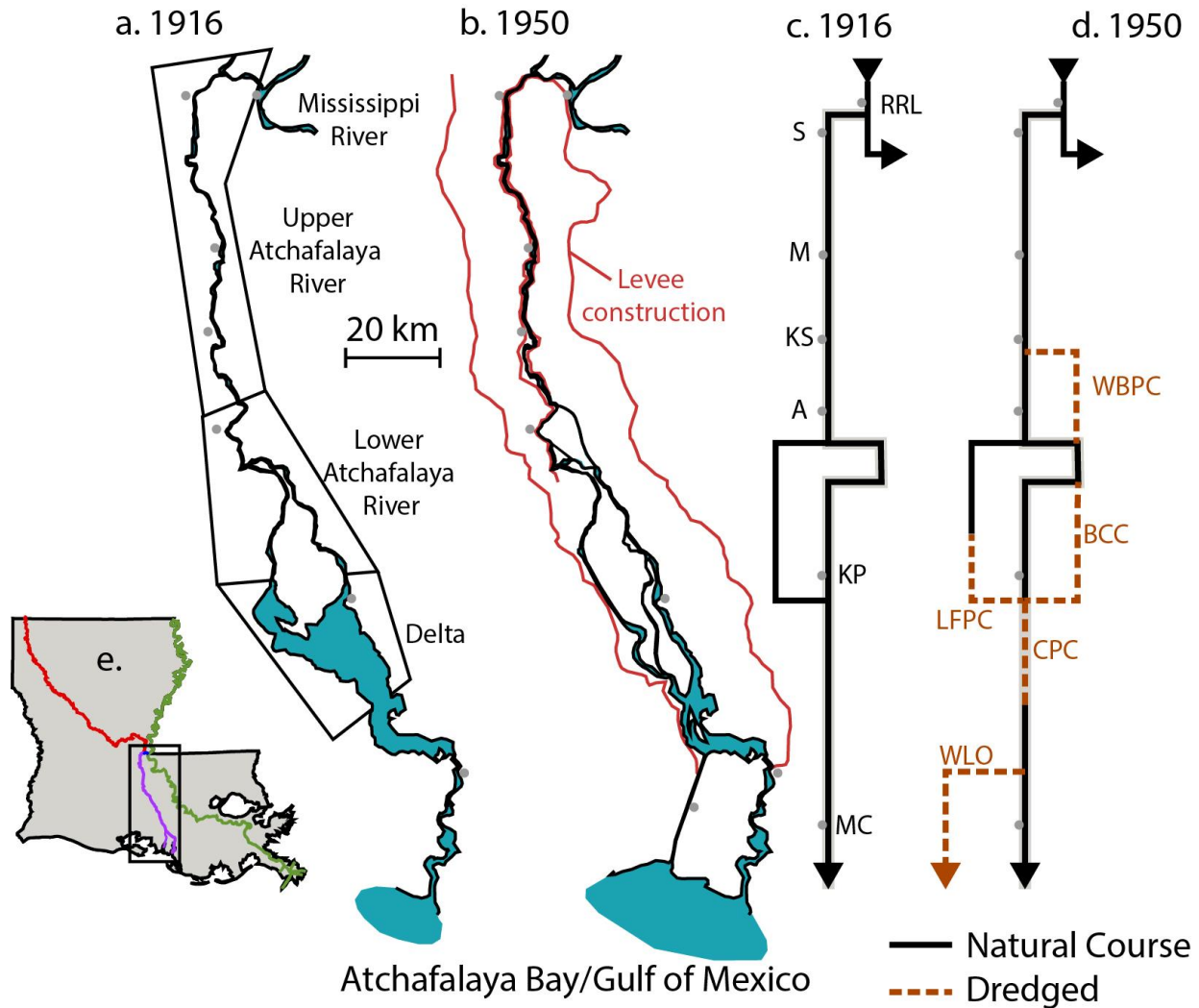
85 ($\pm 1.57\text{IQR}\sqrt{n}$). The period 1916-1931 shows statistically smaller increases than the other periods
86 (notches do not overlap).

87

88 The ORCS was constructed between 1961-1963 because of the rapid increase in discharge down
89 the Atchafalaya River between 1900 and 1950 (Figure 1a; Latimer & Schweitzer, 1951). Over this
90 period, the proportion of water discharge leaving the Mississippi River and flowing into the
91 Atchafalaya River (f_A) grew from about 0.15 in 1900 to about 0.30 in 1950, with an acceleration
92 at some point between 1928 and 1935, when f_A was about 0.18 of annual flows (Figure 1).
93 Increasing f_A over time was interpreted widely as the gradual and inevitable annexation of flow
94 from the established Mississippi channel to produce a new avulsion through the Atchafalaya basin.
95 The annexation was attributed to the gradient advantage of the Atchafalaya River relative to the
96 existing Mississippi channel (240 km vs 496 km), that was thought to increase scouring in the
97 Atchafalaya River (Fisk, 1952; Latimer & Schweitzer, 1951). The diversion angle and partitioning
98 of sediment discharge were considered to have a secondary effect on the discharge increase.

99 The focus of this study is the events that led to the construction of ORCS. By extrapolating the
100 rates of discharge increase and channel enlargement using an unpublished Army Corps internal
101 report by Graves, it was estimated that the Atchafalaya River would annex 40% percent of the
102 Mississippi's discharge between 1965 and 1975, after which the predicted avulsion would be rapid
103 and unstoppable (Fisk, 1952; Latimer & Schweitzer, 1951). The inevitability of the natural
104 avulsion into the Atchafalaya River reached the public consciousness through the famous essay by
105 McPhee (1987).

106 The USACE analyses (Fisk, 1952; Latimer & Schweitzer, 1951) were based on empirical analyses
107 of extensive datasets. However, quantitative analysis of the historic system's hydrodynamics, its
108 forces and motions developed from first principles, has yet to be performed. This is partly because
109 hydrodynamic models were still in their infancy in the early 1950s (e.g. Chow, 1959). Since then,
110 the understanding of avulsion has advanced significantly (Kleinhans et al., 2012; Slingerland &
111 Smith, 2004; Z. B. Wang et al., 1995). However, these advances generally rely on coupled,
112 simplified models of fluid flow, sediment transport, and bed evolution that depart from field
113 measurements of change and limiting their ability to inform a specific system. Hence, we found it
114 compelling to revisit this problem with tools that could quantitatively analyze partitioning based
115 on solid historic measurements, in order to lessen uncertainties and uncover controls of this
116 essential river junction's evolution.



117

118 **Figure 2.** (a and b) maps of the Mississippi and Atchafalaya River System in 1916 and 1950.
 119 Polygons show different regions referred to in the text. Red lines in (b) are artificial levees. (c and
 120 d), Model schematics for flow routing. Arrows show flow sources (arrow tails) and sinks (arrow
 121 heads). Gray circles are hydrograph stations. The pathway which is plotted in Figs 5 and 6 is
 122 outlined in gray. RRL: Red River Landing, S: Simmesport, M: Melville, KS: Krotz Springs, A:
 123 Atchafalaya, KP: Keelboat Pass, MC: Morgan City, WBPC: Whiskey Bay Pilot Channel, BCCO:
 124 Bayou Chene Cutoff, CPC Chicot Pass Channel, Lake Fausse Point Channel. (e) Map of Louisiana,
 125 with the Mississippi River (green), Atchafalaya River (purple), and Red River (red) shown, and a
 126 box demarcating the study area.

127 1.1 Factors potentially influencing partitioning.

128 We construct a relatively simple hydrodynamic model of water discharge through the Mississippi-
 129 Atchafalaya network (Figure 2) to quantitatively assess controls on the rapid increase in
 130 Atchafalaya River discharge. We isolate four potential controls: (i) the widening of the Upper
 131 Atchafalaya River, (ii) evolution of the lower Mississippi River, (iii) the dredging of channels in
 132 Lower Atchafalaya River, and (iv) the progradation of lacustrine deltas into the lakes of the lower
 133 Atchafalaya Basin.

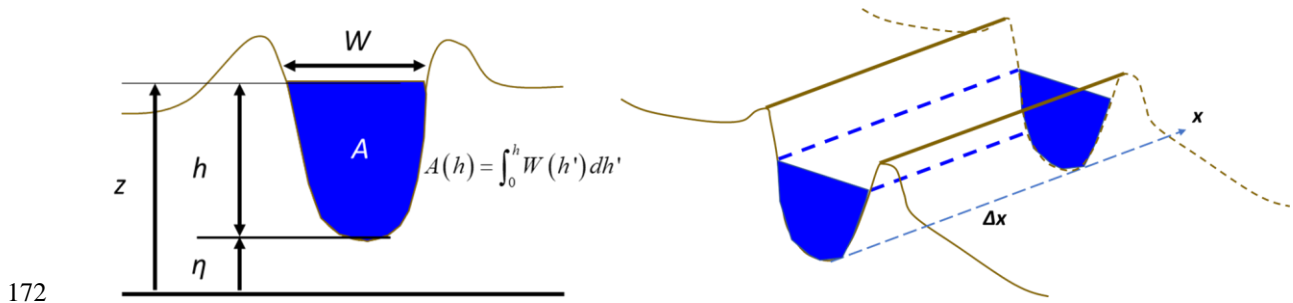
134 The widening and incision of the upper Atchafalaya River between Red River Landing and the
135 Atchafalaya, LA gauge (100 km downstream of Red River Landing; Fig. 2) has been interpreted
136 as the key influence of increasing f_A (Fisk, 1952). Surveys by Latimer and Schweitzer (1951) show
137 channel widening was a relatively consistent process between 1880 and 1950 (median growth
138 $0.016\text{-}0.022\text{ yr}^{-1}$), except 1916-1931 which was remarkably slow (median $-0.0004 \pm 0.0062\text{ yr}^{-1}$;
139 Fig. 1b). The Great Flood of 1927 cannot be isolated from historical surveys, but was the part of
140 the period with the least change. Widening in this region may have been facilitated by a substrate
141 of sand bodies from the historic Mississippi River that were easily erodible (Aslan et al., 2005).

142 The lower Mississippi river was also evolving in the early 20th century. Kesel's (2003) analysis
143 of Mississippi River hydrographic surveys downstream of Red River Landing suggested erosion
144 of the channel thalweg between 1935 and 1948, and interpreted it as the result of a river
145 straightened and steepened by meander cutoffs. Stage-discharge relationships on the Mississippi
146 River between Arkansas City, AR and Red River Landing showed similar reductions in stage for
147 a given discharge between 1930 and about 1945 before increasing gradually after 1945 (Smith &
148 Winkley, 1996). Our analysis of the 1916 and 1949 hydrographic surveys shows that channel
149 thalweg (minimum elevation) did not change significantly, but the cross-sectional area of flow
150 grew slightly, particularly in the final 200 km of the Mississippi River (downstream of New
151 Orleans, LA). See section 5.1 for discussion. Such an increase in Mississippi River cross-
152 sectional area should lead to decreased f_A .

153
154 Between 1932 and 1951, $97 \times 10^6\text{ m}^3$ of sediment dredged from the Atchafalaya River Basin
155 (Latimer and Schweitzer, 1951). While the USACE reports mention dredging activities within the
156 Atchafalaya Basin, they were not considered a significant factor controlling the discharge
157 partitioning (Fisk, 1952), possibly because the dredging was focused in Grand Lake/Six Mile Lake,
158 $>100\text{ km}$ from ORCS. Dredging consisted of significant new channels that did not previously exist.
159 New channels included the Whiskey Bay Pilot Channel (WBPC), The Bayou Chene Cutoff (BCC),
160 and the Chicot Pass Channel (CPC) and the Wax Lake Outlet (WLO; Fig. 2). In the Grand Lake/Six
161 Mile Lake region, navigation channels of the Lake Fausse Point and Grand Lake/Six Mile Lake
162 that were 15-20' deep and 90 m (300 ft) wide. These dredged channels deepened and widened
163 considerably between their dredging and the USACE survey of 1950. This dredging could also
164 influence discharge partitioning. Deepening the Atchafalaya channels should increase f_A .

165 The fourth change to the system that could influence f_A is the growth of the large deltas in Grand
166 Lake in the Atchafalaya Basin. Between 1916 and 1950, about 180 km^2 of lacustrine delta
167 deposits accumulated in Grand Lake (Roberts et al., 1980; Tye & Coleman, 1989). Such deposits
168 should act to reduce cross sectional area of flow and decrease f_A .

169

170 **2 Methods and Data**171 **2.1 Model**

172
173 **Figure 3.** Schematic diagrams of hydrodynamics model. (a) Definition of cross-section area; (b)
174 1-D long profile of river channel with cross-sections aligned downstream.

175 Water discharge can be modeled through the Mississippi-Atchafalaya channel network using the
176 backwater equation for steady, non-uniform (gradually varied) flow (Chow, 1959; Parker, 2004).
177 This system includes channels that vary from narrow and prismatic (in the Upper Atchafalaya
178 River) to those with significant flow outside the channel (in the Atchafalaya Delta). We thus
179 provide a detailed derivation of the backwater equation for an arbitrary cross-section. We start
180 from 1-D shallow water equation for arbitrarily-shaped cross-sections (Ying et al., 2004), which
181 has been tested in channels with abrupt width contraction and expansion and trans-critical slope
182 channel (Ying et al., 2004; Ying & Wang, 2008):

$$183 \quad \frac{\partial A}{\partial t} + \frac{\partial Q}{\partial x} = 0 \quad (3)$$

$$184 \quad \frac{\partial Q}{\partial t} + \frac{\partial(Q^2/A)}{\partial x} = gA \left(-\frac{\partial z}{\partial x} - S_f \right) \quad (4)$$

185 where t is time [T]; x is streamwise spatial distance [L]; g is gravitational acceleration [LT^{-2}]; A
186 is the wetted cross-sectional area [L^2]; Q is the water discharge [L^3T^{-1}]; $z = \eta + h$ is the water
187 surface elevation where η is the bed elevation and h is the water depth at the channel thalweg
188 [L]; $S_f = C_f u |u| / (gA / \Gamma)$ is the frictional slope where C_f is the resistance coefficient, u is the
189 cross-sectionally averaged velocity $u = Q / A$ [LT^{-1}], and Γ is the wetted perimeter [L].

190
191 For the steady, non-uniform flow in a non-bifurcating reach, Eqs. (3-4) reduce to

$$192 \quad \frac{\partial Q}{\partial x} = 0, \quad (5)$$

$$193 \quad \frac{\partial h}{\partial x} = S - S_f - \frac{1}{gA} \frac{\partial(Q^2/A)}{\partial x} \quad (6)$$

194 where $S = -\partial \eta / \partial x$ is the channel bed slope [-].

195

196 Substituting Eq. (5) to Eq. (6), we obtain

$$\frac{\partial h}{\partial x} = S - S_f + \frac{u^2}{gA} \frac{\partial A}{\partial x}. \quad (7)$$

Note that $\frac{\partial A}{\partial x} = \frac{\partial A}{\partial h} \frac{\partial h}{\partial x} = W \frac{\partial h}{\partial x}$, where W is channel width at the water surface as shown in Fig.

3. Hence, Eq. (7) turns to $\frac{\partial h}{\partial x} = S - S_f + \frac{u^2}{gA/W} \frac{\partial h}{\partial x}$ and since Froude number has the following

relation $F^2 = \frac{u^2}{gA/W}$, we thus obtain

$$\frac{\partial h}{\partial x} = \frac{S - S_f}{1 - F^2}, \quad (8)$$

where $S_f = C_f u |u| / (gA / \Gamma)$.

This formulation has been used as a simple way to estimate flow dynamics on large rivers (Lamb et al., 2012; Nittrouer et al., 2012; Viparelli et al., 2015; Z. B. Wang et al., 1995), but has not been previously used to model a network of many interacting channel reaches. In order to solve for h , A , u , and Q , throughout the channel network, it is broken into non-branching reaches i joined at nodes representing bifurcations and confluences. Under Froude-subcritical conditions ($F^2 < 1$), the boundary conditions Q_i and the downstream water depth allow Eq. 8 to be solved along each reach. Reaches are linked by discharge constraints. At a node where an upstream channel a bifurcates into two channels b and c , we specify $Q_a = Q_b + Q_c$, with the discharge partitioning fraction defined as $f_b = Q_b / Q_a$. At a confluence node where two channels d and e flow together to form a single channel g , $Q_d + Q_e = Q_g$. Although upstream flow ($Q_i < 0$) is potentially possible in some networks, we stipulate $Q_i \geq 0$ in this study because tidally averaged flows are always unidirectional through this system.

In addition to bathymetric transects summarized in Section 2.2, two hydraulic boundary conditions are required for a model run. First, upstream discharge (Q_0) is specified at the Mississippi River at Red River Landing (RRL; Fig. 2). The Red River also provides discharge to the system, and can be as large as 10% of the Mississippi River's discharge. However, we neglect it here because it enters the Atchafalaya River upstream of Simmesport, where Atchafalaya River discharge and f_A is measured by Latimer and Schweitzer (1951). Second, the boundary condition of water surface elevation is applied at each channel terminus where the network meets sea level, ($z = 0$ m MSL).

The model is solved by iteratively finding discharge partitioning values f_i that minimize disparities in water surface elevation at each bifurcation. (1) An initial set of discharge partitionings f_{i0} is chosen; (2) based on f_{i0} , the water surface is solved using Eq. (8); (3) at each bifurcation, the water surface elevation at the downstream end of the upstream reach (z_{of}) is set equal to the water surface elevation of one of the reaches d or e (z_{1d} , z_{1e}); (4) when flow has been solved throughout the network, the sum of squared difference in water surface elevation $E = \sum \Delta z^2 = \sum (z_{1d} - z_{1e})^2$ is iteratively minimized using the quasi-newton optimization technique found in MATLAB (Shanno, 1970). When a minimum of E is found, each bifurcation will have a single water surface elevation and the water surface will be nearly continuous throughout the channel network. For model runs described here, final solutions of f_i produce very small absolute water differences ($E < 10^{-6}$ m²)

232 ensuring near-continuity state of the water surface across the network, and a plausible
233 reconstruction of fluid flow.

234 2.2 Hydrographic Survey Data and Network Models

235 This study relies on detailed bathymetric and hydrological measurements collected by the US
236 Army Corps of Engineers. Hydrographic surveys of transects were digitized from before and after
237 the significant increase in discharge by the Atchafalaya River for validation (see section 3.1).
238 Synthetic models focused on specific changes between 1916 and 1950 were then used to test
239 hypotheses about the controls on Mississippi-Atchafalaya partitioning. A library of these
240 hydrographic surveys and models are included in the supplementary material.

241 The pre-annexation model (R16) consisted of the most recent surveys prior to significant dredging
242 that began in 1932. This model contained five reaches (Fig. 2c), with bifurcations at Red River
243 Landing (RRL) and within the lower Atchafalaya River. The Atchafalaya River portion of this
244 model consisted of hydrographic surveys collected between 1910 and 1930 published in Latimer
245 and Schweitzer (1951, Vol. 3). The mean transect spacing was 3.5 km. The Mississippi River
246 portion of the model was the 1913 Mississippi River Hydrographic Survey (USACE, 1915)
247 between the Mississippi-Atchafalaya Bifurcation at Old River, and Venice, LA, where significant
248 flow begins leaving the main channel, 17 km upstream of head of passes. The mean transect
249 spacing was 0.3 km.

250 The post-annexation model (R50) consisted entirely of hydrographic surveys collected after the
251 end of significant dredging in 1950. This model contained 11 reaches (Fig. 2d) with five
252 bifurcations. The additional bifurcations relative to R16 were due to the Whiskey Bay Pilot
253 Channel, Bayou Chene Cutoff, and Wax Lake Outlet. Dredging from the Lake Fausse Pointe Cut
254 and Atchafalaya Basin Main Channel altered existing transects. The Atchafalaya River surveys are
255 also published in Latimer and Schweitzer (1951, Vol. 3). The Mississippi River portion of this
256 model was the 1949 Mississippi River Hydrographic Survey (USACE, 1950) between Old River
257 and Venice.

258 Stage-discharge relationships were recorded at seven locations, from Red River Landing to
259 Morgan City, Louisiana (Fig. 2c; Latimer and Schweitzer, 1951). Such relationships were recorded
260 at various years between 1880 and 1950. The relationship from about 1916 served as a pre-
261 annexation validation, and the relationship from about 1950 served as the post-dredge validation.

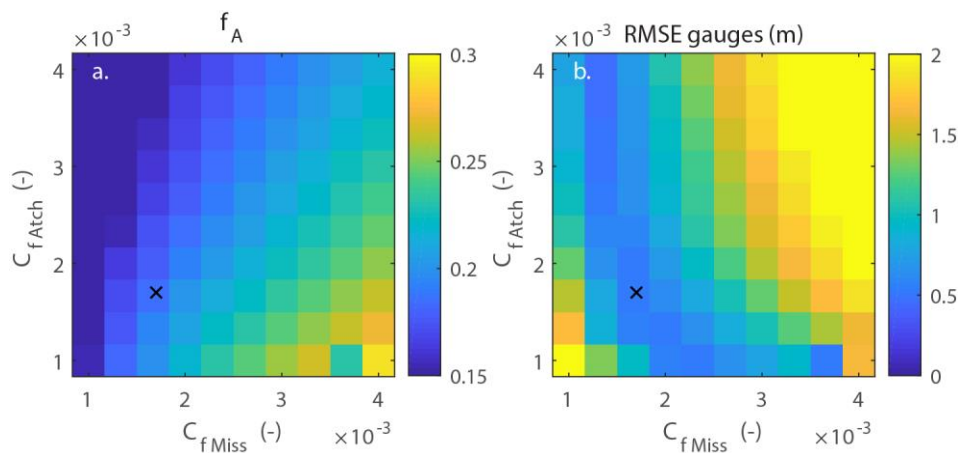
262 To isolate the effect of dredging within the basin, several hydrodynamic models were constructed
263 that altered certain aspects of the two baseline models. Model R16D isolated the effect of dredging
264 in the Atchafalaya River by adding the planned dredging within the Atchafalaya Basin, including
265 the new channels to the 16M model (available in Latimer and Schweitzer 1951, Vol. 3). These
266 cross-sections were generally smaller than the same cross-sections in 1950 because significant
267 erosion and widening occurred after dredging, similar to R50, R16D had 11 reaches. Model R16A
268 isolated the effect of channel widening in the Atchafalaya Basin by taking the R16 model but
269 adding the 1950 cross sections of the Upper Atchafalaya River where channel width had
270 significantly increased. Model R16M isolated the influence of changes in the Mississippi River
271 over the study period by taking the R16 model and exchanging the 1949 Mississippi River
272 hydrographic survey. Finally, Model R16GL isolated the effect of sediment accumulation within

273 Grand Lake by taking model R16 and exchanging R50 transects only within Grand Lake. Models
 274 R16A, R16M, and R16GL maintained the same transect structure as R16.

275 3. Results

276 3.1 Validation

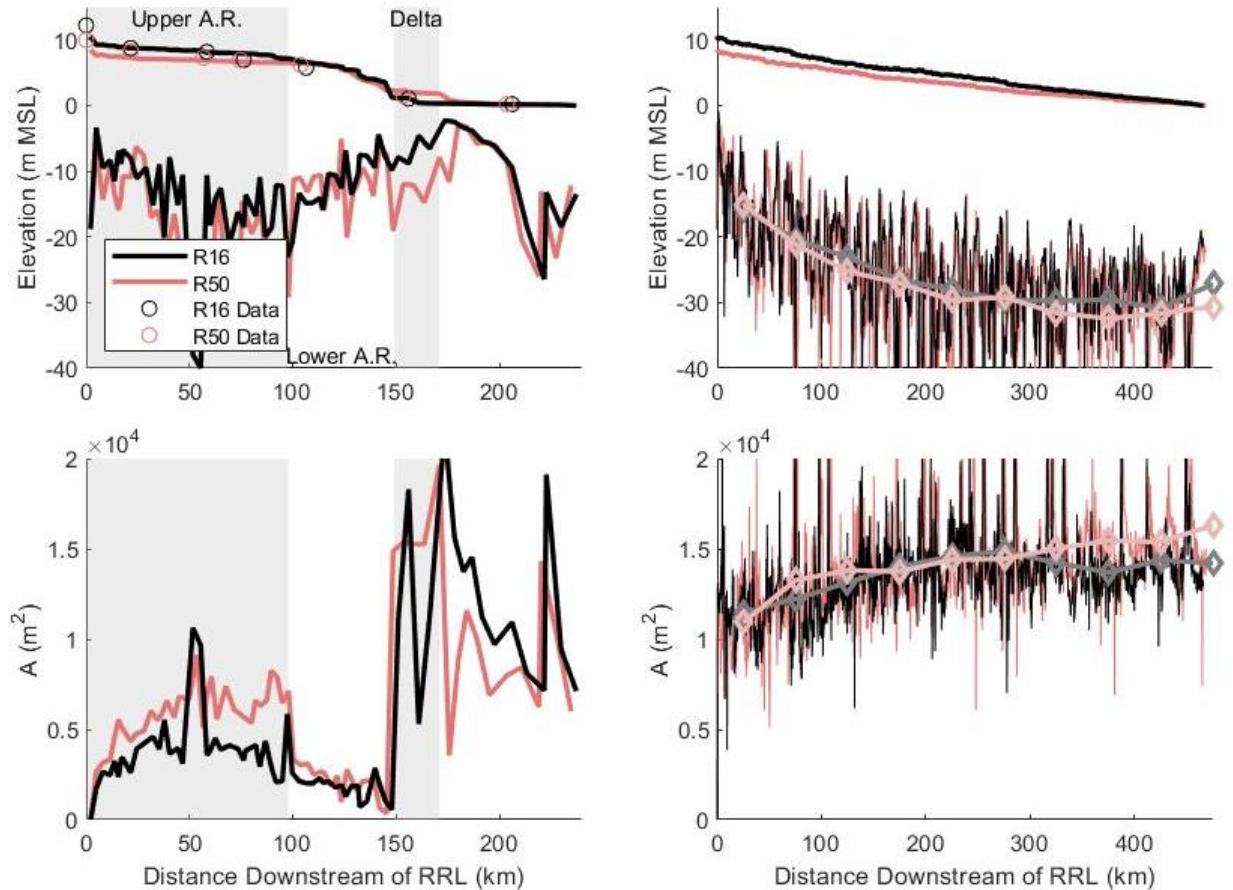
277 The hydrodynamic model was validated against (a) the measured discharge partitioning ($f_A \sim 0.18$;
 278 Fig. 1) and (b) measured stage-discharge curves. An upstream discharge of $Q_0 = 20,000 \text{ m}^3/\text{s}$ was
 279 used throughout the validation and modeling process because it corresponds closely to the
 280 Mississippi Rivers average annual discharge between 1900 and 1960 ($18,300 \text{ m}^3/\text{s}$; Latimer and
 281 Schweitzer, 1951). Preliminary models were run with discharges ranging from $15,000\text{-}35,000 \text{ m}^3/\text{s}$
 282 which showed gradually increasing f_A with increasing Q_0 , consistent with Edmonds (2012).
 283 Variable flow discharge has an important control on centers of erosion and deposition and
 284 influences general models of avulsion (Chadwick et al., 2019; Ganti, Chadwick, Hassenruck-
 285 Gudipati, et al., 2016; Lamb et al., 2012). However, our focus is on the recorded increase in average
 286 annual flows to the Atchafalaya River, with the changing network set from data. For this reason,
 287 we leave the modeling of variable discharge through the system to future work.



288

289 **Figure 4.** (a) partitioning of flow in 1916 and (b) root-mean-square error of the 7 stage-discharge
 290 gauges were used to determine an ideal combination of friction factor (C_f) in the Mississippi River
 291 (x axes) and Atchafalaya River (y axis). The black x shows the friction factors that were chosen
 292 for modeling. Results shown for upstream discharge $Q_0 = 20,000 \text{ m}^3/\text{s}$.

293 Model R16 was run for a variety of friction factors in both the Mississippi River (C_{f_Miss}) and the
 294 Atchafalaya network (C_{f_Atch}) ranging from 0.001 and 0.004 (Figure 4). Partitioning (f_A) increased
 295 with increasing C_{f_Atch} and decreasing C_{f_Miss} . The root-mean-square error between measured and
 296 modeled gauge heights reached a minimum of 0.56 m for intermediate C_f , which is about 3% of
 297 18 m average flow depth. We chose $C_{f_Atch} = C_{f_Miss} = 0.0017$ for this study which is consistent
 298 with the direct measurement at Tarbert Landing, Mississippi River (Karim, 1995) and the
 299 prediction of the prevailing resistance relation (Engelund & Hansen, 1967). It is slightly smaller
 300 than friction factors used to model the modern Mississippi river by Nittrouer et al. (2012; 0.003 -
 301 0.007), but closer to the value used by Edmonds (2012; 0.0023).



302

303 **Figure 5.** Results for models R16 (black) and R50 (red) under upstream discharge $Q_0 = 20,000$
 304 m^3/s . Panels a (thalweg depth and water surface) and c (cross-sectional area) show the primary
 305 path through the Atchafalaya River network (see Fig. 2c,d). Circles show hydrograph heights for
 306 corresponding discharges. Panels b and d show the lower Mississippi River. Fine lines show
 307 thalweg elevation and cross sectional area for every transect. Thick lines and diamonds show 50
 308 km averages.

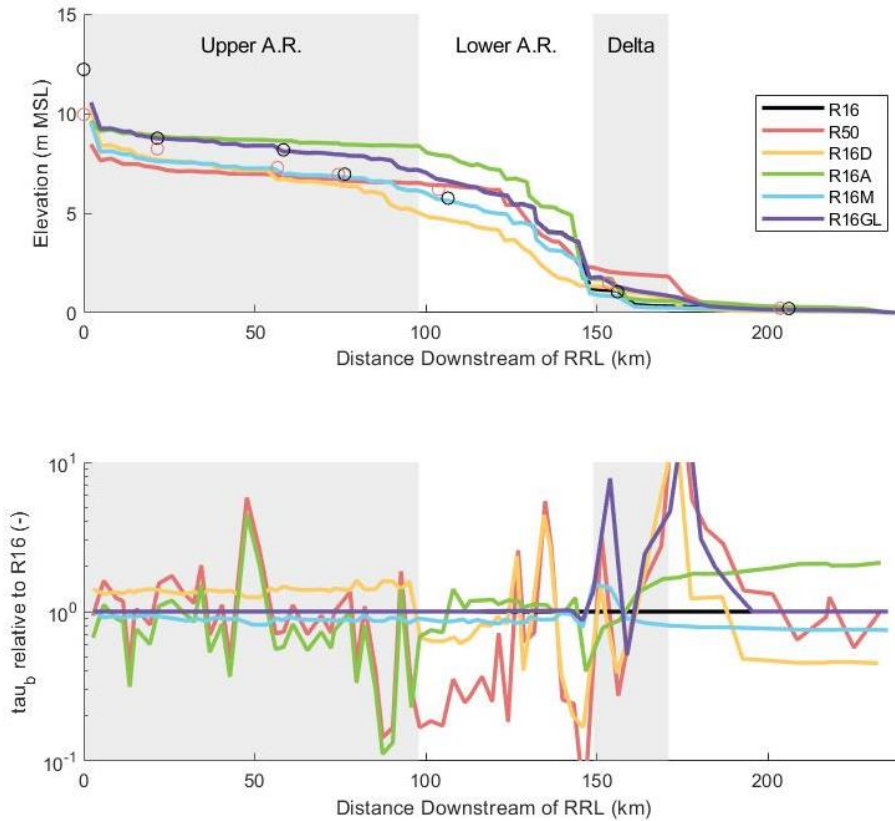
309

310 Using the calibrated C_f values, discharge partitioning f_A between the Mississippi and Atchafalaya
 311 Rivers was modeled as 0.185 for R16 and 0.279 for R50. These results compare well with data
 312 showing f_A between 0.18-0.22 in 1932 and 0.28-0.32 in 1950. Model runs R16 and R50 and
 313 hydrograph data (Figure 5, Table 1) show a similar water surface profile for average annual
 314 discharge to the system. The large, low-slope channel in the upper Atchafalaya River transitions
 315 to the smaller, higher-slope channel in the lower Atchafalaya River, producing a concave down
 316 “M2 curve” (Chow, 1959) from 110-130 km downstream of Red River Landing. At the transition
 317 to the wide and shallow Grand Lake, slopes are significantly reduced again, producing a concave
 318 up “M1 curve”.

319 The post-annexation model (R50) and data differ from their pre-annexation counterparts (R16) in
 320 terms of their slopes in the upper Atchafalaya River (for the same Q_0 , but 51% increase in Q in the

321 Atchafalaya River; Table 1). Hydrograph data show that the stage at Red River Landing dropped
 322 2.2 m, consistent with the modeled 2.1 m drop. Relatedly, slopes in the upper Atchafalaya River
 323 (measured over 104 km between RRL and Atchafalaya, LA) dropped 31% (hydrograph data) to
 324 41% (models).

325 3.2 Partitioning Attribution



326
 327 **Figure 6.** (a) Water surface profiles along the primary pathway through the Atchafalaya Basin (see
 328 Fig. 2) for all models. (b) Shear stress ($\tau_b = \rho C_f F^2$) along each transect divided by the shear
 329 stress from run R16. Note logarithmic y axis.

330 Synthetic channel networks of the Mississippi-Atchafalaya System (described in Section 2.2) were
 331 used to test how various changes between 1916 and 1950 influenced discharge partitioning (Figure
 332 6). Two important aspects of the simulations are considered. First, model f_A is compared to the
 333 results from R16 and R50 (f_A of 0.185 and 0.279 respectively) in order to assess the control on
 334 discharge partitioning. Second, the stage change at Red River Landing is compared to the
 335 simulated stages (10.5 m and 8.4 m respectively).

336 Model R16A showed $f_A = 0.271$, or 91% of the required discharge increase from R16 to R50.
 337 However, the stage at RRL dropped to just 9.6 m, explaining only 43% of the total stage drop.
 338 Model R16D produced a partitioning of $f_A = 0.197$, explaining just 13% of the modeled change
 339 between R16 and R50. The stage at RRL dropped to 10.4 m, which was only 26% of the stage

340 change there. Change was focused where dredging of new channels occurred in the lower,
341 Atchafalaya River and produced more gradual water surface slopes.

342 Model R16M produced $f_A = 0.161$, the only model that reduced f_A relative to R16. This is because
343 minor increases to channel cross-sectional area of the Mississippi River acted to reduce slopes in
344 the Mississippi River and stage at RRL to 9.5 m, thereby reducing discharge to the Atchafalaya
345 River. The stage reduction was 47% of the total reduction in stage between R16 and R50.

346 Despite the growth of significant lacustrine delta deposits between 1916 and 1950, model R16GL
347 produced essentially the same discharge partitioning and RRL stage as R16. This suggests that
348 they had little to no impact on the discharge partitioning at the Mississippi-Atchafalaya bifurcation.

Model	f_A (-) ($Q_0=20,000$ m^3/s)	Upper A.R. Slope ($\times 10^{-5}$)	Lower A.R. Slope ($\times 10^{-5}$)	z at RRL (m MSL)	Fraction of f_A change explained by model	Mean τ_b , Upper A.R. (N/m^2)
Data 1932	0.18-0.22	5.71	10.02	12.2		
Data 1950	0.28-0.32	3.96	9.08	9.96		
R16	0.185	3.48	11.45	10.5		2.3
R50	0.279	2.04	8.32	8.4		1.9
R16D	0.197	5.49	7.30	10.4	13%	3.2
R16A	0.271	1.32	13.07	9.6	91%	1.4
R16M	0.161	3.50	9.94	9.5	-26%	2.1
R16GL	0.185	3.50	10.06	10.5	0%	2.3

349 **Table 1.** Hydrograph data and hydrodynamic model outputs for the Mississippi-Atchafalaya
350 system.
351

352 **5 Discussion**

353 **5.1 Attribution to the Atchafalaya partial avulsion**

354 The proposed numerical model quantitatively depicted the increase in the proportion of discharge
355 down the Atchafalaya River between 1916 and 1950 well (Figure 5), and clearly showed that it
356 was the result of several simultaneous processes. Erosion of the Upper Atchafalaya River

357 produced the largest increase in f_A . This is consistent with the original assessment of the Army
358 Corps of Engineers (Fisk, 1952). However, dredging in the Atchafalaya river network and
359 changes in the Mississippi river also influenced the system, while the lacustrine deltas did not.

360 The increase of cross-sectional area in some parts of the lower Mississippi River between 1913
361 and 1951 (the years of the USACE surveys) has not been previously linked to the Mississippi-
362 Atchafalaya diversion. We attribute roughly half of the 2 m stage reduction (47% of total stage
363 reduction) at Red River Landing to lower Mississippi River changes (Table 1). The increase in
364 cross-sectional area occurred in two locations. First, 50-150 km downstream of Red River
365 Landing (roughly between St. Francisville and Plaquemine, LA) in the fully alluvial reach of the
366 river, and >300 km downstream (downstream of New Orleans, LA; Figure 4) in the alluvial-
367 bedrock reach of the river (Viparelli et al., 2015). While reach-averaged increases to cross-
368 sectional area were between 5 and 15% (diamonds Fig. 3d), they impacted f_A by reducing water
369 surface slopes, and therefore the stage at Red River Landing. Lower Mississippi River erosion
370 during the study period is consistent with previous studies (Kesel, 2003; Smith & Winkley,
371 1996). However, it is worth noting that since this period, the lower Mississippi River has had
372 periods of both aggradation and degradation (Galler et al., 2003; Knox & Latrubesse, 2016; B.
373 Wang & Xu, 2016, 2018; Wu & Mossa, 2019). Had the lower Mississippi River been
374 aggradational during the study period, f_A may have increased more rapidly.

375 Dredging in the lower Atchafalaya River basin acted to increase discharge, producing 13% of the
376 measured increase between 1916 and 1950. However, there are remarkable differences in
377 hydrodynamics comparing the widening (R16A) or dredging (R16D) models. When widening is
378 considered in the absence of dredging, discharge increases can only be accommodated by
379 increased slopes in the lower Atchafalaya River (R16: 11.4×10^{-5} , R16A 13.1×10^{-5}) which
380 produced higher stages and lower slopes in the upper Atchafalaya River (Fig. 6a). In contrast,
381 when dredging is considered in the absence of widening (R16D), reduced slopes in the lower
382 Atchafalaya River are possible (R16D: 7.3×10^{-5}), which lead to reduced stages and higher slopes
383 in the upper Atchafalaya River. The effects on shear stress in the upper Atchafalaya River ($\tau_b =$
384 $\rho C_f u^2$) are remarkable (Fig. 6b). Shear stress is reduced by 39% due to widening (2.3 to 1.4
385 N/m^2 ; Table 1) despite a 46% discharge increase. In contrast, the 6% discharge increase of R16D
386 increases shear stress by 39% (2.3 to 3.2 N/m^2). Hydrograph data offer a consistent story.
387 Between 1916 and 1950, the water surface slope decreased 31% (5.71×10^{-5} to 3.96×10^{-5} ;
388 Figure 6a) in the upper Atchafalaya River but decreased only 9% in the lower Atchafalaya. The
389 erosion and increased cross-sectional area of the upper Atchafalaya River are presumably the
390 result of heightened shear stresses, and the period of dredging showed consistently large rates of
391 cross-sectional area increase (Fig. 1b). Our results show that a negative feedback between
392 widening and shear stress in the upper Atchafalaya River could limit widening, but increased
393 channelization in the lower Atchafalaya could remove this feedback and potentially lead to
394 greater widening.

395 Dredging appears to have transformed the lower Atchafalaya River. The pre-existing channels
396 through this region did not erode during the study period (Fig. 5a,c), while dredged channels
397 quickly became dominant. Prior to 1934, the Whiskey Bay Pilot Channel (WBPC) did not exist,
398 and discharge was accommodated by 2-4 small channels. While many of these channels enlarged
399 between 1932 and 1950 (Latimer and Schweitzer, 1951), dredging immediately diverted 1340
400 m^3/s (34%) from the lower Atchafalaya River (inferred from R16D), continued to grow after

401 initiation through subsequent erosion, diverting 3205 m³/s (57%) from the lower Atchafalaya
402 River by 1950 (from R50). It is presently the dominant channel through this part of the basin. It
403 is unclear how the lower Atchafalaya River network would have evolved in the absence of
404 dredging, although a primary channel is eventually established in many depositional avulsions
405 (Slingerland & Smith, 2004). However, a deeply incised, relatively straight, primary channel
406 through the system like the dredged network (Fig. 1) seems unlikely to have formed, especially
407 in a 16 year period.

408 Finally, the growth of 180 km² of deltas in Grand Lake did not factor in partitioning or stage at
409 Red River Landing. These deltas did act to reduce channel cross sectional area and increase stage
410 and slopes for R16GL by 0.7 m relative to R16 within the delta area (148-180 km downstream of
411 RRL; Fig. 5a). However, the water surface of the R16 and R16GL collapsed on one another in
412 the lower Atchafalaya River and were similar at all points above. Numerical models of
413 backwater flow with smoothly varying bed topography show that stage changes decay
414 asymptotically (Chadwick et al., 2019; Ribberink & Van Der Sande, 1985). However, the steep
415 water surface slopes (locally 5.2×10^{-4} , $F^2 = 0.2$) associated with the M2 curve in the lower
416 Atchafalaya River overwhelmed such gradual trends.

417 **5.2 Limitations and Advantages**

418 The models considered here were constructed in a deliberately simple manner so that they could
419 be adequately run with the available historic data and allow several hypotheses to be tested.
420 While the present study is enough to compare well with validation data and produce first order
421 attribution, more complex models are necessary for engineering grade applications, particularly
422 for coupling bed evolution and flows that are not averaged at a transect. Globally, coastal
423 systems are evolving under simultaneously active natural and human drivers (Hoitink et al.,
424 2020; Lazarus & Goldstein, 2019). The methods presented here are suitable for cases where
425 survey data exists in order to further develop the understanding of recent, current and future
426 channel network evolution in coastal systems worldwide.

427 **5.3 Implications**

428 This study facilitates a comparison to the current understanding of avulsion controls. The “setup”
429 for avulsion was small, but consistent with prevailing models. Within 10 km of Red River
430 Landing in 1916, the Mississippi River had a spatially averaged water surface elevation (for $Q_0 =$
431 20,000 m³/s) of 10.2 m MSL and bed elevation of -11.3 m MSL. Compared to the minimum
432 floodplain elevation in the region (8 m; Aslan et al. 2005), the fraction of flow depth above the
433 flood plain (the superelevation ratio) was 0.1. This value is smaller than the mean superelevation
434 ratio at avulsions of the Assiniboine River (0.65; Mohrig et al., 2000), Bayou Lafourche (~0.1;
435 Törnqvist & Bridge, 2002) and laboratory experiments (0.3; Ganti et al., 2016; 0.9; Martin et al.,
436 2009), but each dataset records avulsions with this superelevation with at least 5% frequency. On
437 the other hand, we find it remarkable that the lower Mississippi River was slightly erosional
438 during the pivotal 34 year of discharge increase (Figure 1). This contrasts with prevailing models
439 which expect deposition in the main channel before and during avulsion to drive the flow
440 reorganization (Ganti, Chadwick, Hassenruck-Gudipati, et al., 2016). Rather than “choking” the
441 main channel, the key control on discharge increase shown was the enlargement of the upper
442 Atchafalaya River, consistent with an incisional avulsion model (Hajek & Edmonds, 2014;
443 Slingerland & Smith, 2004), where the excavation of the new channel is of primary importance.

444 The sandy, easily erodible deposits found in the upper Atchafalaya River region (Aslan et al.,
445 2005), and the dredging at Old River between 1878 and 1937 (Mossa, 2013) may have facilitated
446 this growth. While the delta deposits in Grand Lake are a significant depositional element, their
447 position downstream of the M2 curve and the channels dredged through them prevented them
448 from hindering discharge increase in the way that depositional wedges in progradational
449 avulsions often do (Slingerland & Smith, 2004). There is good evidence that the location of
450 avulsions in large channels with backwater flow scales with the Backwater Length; the average
451 flow depth divided by the energy slope (Chatanantavet et al., 2012; Ganti, Chadwick,
452 Hassenruck-Gudipati, et al., 2016; Jerolmack & Swenson, 2007; Lane, 1957). Even so, avulsion
453 locations vary by at least a factor of 3 around this scale (J. B. Shaw & McElroy, 2016), and the
454 understanding of this variation remains limited. Although the Atchafalaya River's course is set in
455 this study, it reveals distinct behavior of this particular system that could influence partitioning
456 and avulsion elsewhere.

457 Our work has important implications for management of the Mississippi-Atchafalaya system,
458 and for flow management in complex networks in general. The Old River Control Structure
459 currently regulates discharge partitioning in the system. However, stress on this regulation has
460 occurred in the past, notably in 1973 when the Low Sill structure was damaged during a large
461 flood (Mossa, 2016), and evolution of the channel network could impart additional stress. Large-
462 scale coastal restoration efforts are being undertaken to make coastal Louisiana resilient to
463 hazardous changes in the coming century (Bentley et al., 2016; CPRA, 2017; Gasparini & Yuill,
464 2020). These plans appear to assume constant future partitioning at ORCS, but may benefit from
465 optimizing f_A to the wide range of restoration objectives (e.g. Kenney et al., 2013; Peyronnin et
466 al., 2017).

467
468 For the management of flow through complex networks in general, our work stresses several
469 things. First (and most intuitively), changes closer to a channel branch, such as the widening of
470 the upper Atchafalaya River, affect the hydrodynamics there more significantly. Second, small
471 changes to the largest channels of the system can significantly affect the smaller changes in the
472 network. The minute changes to the lower Mississippi River acted to reduce stage at RRL, and
473 could have potentially reduced f_A , had the Atchafalaya Basin not evolved. Third, this study
474 shows that reaches like the lower Atchafalaya River - which have few or small channels, high
475 water surface slopes, and naturally produce an M2 curve under non-flood discharges - can act as
476 a "choke point" in the system. Increased connectivity across these reaches will reduce stage and
477 increase shear stress upstream. Finally, apparently large changes downstream of these reaches
478 (such as delta deposition) may not be propagated upstream in a significant way.

479 **6 Conclusions**

480 We present evidence that the rapid increase in water discharge into the Atchafalaya River
481 between 1916 and 1950 can be attributed to three important changes to the Mississippi-
482 Atchafalaya system over that period. First the relatively consistent widening of the upper
483 Atchafalaya River produced significant increases in the fraction of water discharge entering the
484 Atchafalaya River, as was originally interpreted by the US Army Corps of Engineers (Fisk,
485 1952). Significant channel dredging in the lower Atchafalaya River further also increased
486 partitioning by increasing connectivity through a steep, low connectivity reach, potentially
487 increasing shear stresses in the eroding channel upstream. The subtle erosion of the lower

488 Mississippi River acted to reduce stage at Red River Landing, and reduce partitioning. The
 489 extensive lacustrine deltas that formed in the lower Atchafalaya Basin did not significantly
 490 influence partitioning. These results demonstrate the natural and anthropogenic forcings on a
 491 large complex channel network can be isolated, and quantitatively evaluated in a manner that can
 492 aid management of important sites.

493 **Acknowledgments, Samples, and Data**

494 This research project was conceived by J.S. Data digitization was performed by G.M. and K. M.,
 495 with additional help from Micheal Amos and J.S. Important methodological updates were
 496 provided by H.M. Final analyses were performed primarily by J.S., with important contributions
 497 by K.M. and G.M., a preliminary version of this work was published as an M.S. thesis by
 498 McCain (2016). All authors contributed to writing, with primary contributions by J.S. Data and
 499 MATLAB code required to reproduce this study is available at 10.6084/m9.figshare.12440279.
 500 Support was provided by the DOE under DESC0016163 to JS. The authors declare no real or
 501 perceived financial interests in this study.

502 **Appendix: Notation**

503	A	Cross-sectional Area of a channel below the water surface (L^2)
504	A.R.	Atchafalaya River
505	M.R.	Mississippi River
506	C_f	Dimensionless friction factor (-)
507	E	Error function for optimization (L^2)
508	F	Froude number (-)
509	f_i	Fraction of upstream flow entering channel reach i
510	f_A	Fraction of Q_0 entering the Atchafalaya River.
511	g	Gravitational acceleration (L/T^2)
512	Γ	Wetted perimeter at a cross section (L)
513	h	Water depth from water surface to minimum channel elevation (L)
514	η	minimum bed elevation, thalweg elevation (L relative to mean sea level; MSL)
515	Q	Discharge (L^3/T)
516	Q_0	Input water discharge upstream of Red River Landing (L^3/T)
517	S	Bed slope ($-\partial\eta/\partial t$; -)
518	S_f	Frictional slope (-)
519	t	Time (T)
520	u	Water velocity, averaged across A (L/T)
521	W	Channel width at water surface (L)
522	x	Downstream coordinate (L)
523	z	Water surface elevation (L relative to mean sea level; MSL)

524

525 **References**

- 526 Aslan, A., Autin, W. J., & Blum, M. D. (2005). Causes of river avulsion: insights from the late Holocene avulsion
 527 history of the Mississippi River, USA. *Journal of Sedimentary Research*, 75(4), 650–664.
- 528 Bain, R. L., Hale, R. P., & Goodbred, S. L. (2019). Flow Reorganization in an Anthropogenically Modified Tidal
 529 Channel Network: An Example from the Southwestern Ganges-Brahmaputra-Meghna Delta. *Journal of*
 530 *Geophysical Research: Earth Surface*, 0(ja). <https://doi.org/10.1029/2018JF004996>

- 531 Batker, D., de la Torre, I., Costanza, R., Day, J. W., Swedeen, P., Boumans, R., & Bagstad, K. (2014). The Threats
532 to the Value of Ecosystem Goods and Services of the Mississippi Delta. In J. W. Day, G. P. Kemp, A. M.
533 Freeman, & D. P. Muth (Eds.), *Perspectives on the Restoration of the Mississippi Delta: The Once and*
534 *Future Delta* (pp. 155–173). Dordrecht: Springer Netherlands. [https://doi.org/10.1007/978-94-017-8733-](https://doi.org/10.1007/978-94-017-8733-8_11)
535 [8_11](https://doi.org/10.1007/978-94-017-8733-8_11)
- 536 Bentley, S. J., Blum, M. D., Maloney, J., Pond, L., & Paulsell, R. (2016). The Mississippi River source-to-sink
537 system: Perspectives on tectonic, climatic, and anthropogenic influences, Miocene to Anthropocene. *Earth-*
538 *Science Reviews*, 153, 139–174. <https://doi.org/10.1016/j.earscirev.2015.11.001>
- 539 Blum, M. D. (2019). Organization and reorganization of drainage and sediment routing through time: the
540 Mississippi River system. *Geological Society, London, Special Publications*, 488.
541 <https://doi.org/10.1144/SP488-2018-166>
- 542 Blum, M. D., & Roberts, H. H. (2012). The Mississippi Delta Region: Past, Present, and Future. *Annual Review of*
543 *Earth and Planetary Sciences*, 40(1), 655–683. <https://doi.org/10.1146/annurev-earth-042711-105248>
- 544 Chadwick, A. J., Lamb, M. P., Moodie, A. J., Parker, G., & Nittrouer, J. A. (2019). Origin of a Preferential Avulsion
545 Node on Lowland River Deltas. *Geophysical Research Letters*, 46(8), 4267–4277.
546 <https://doi.org/10.1029/2019GL082491>
- 547 Chatanantavet, P., Lamb, M. P., & Nittrouer, J. A. (2012). Backwater controls of avulsion location on deltas.
548 *Geophysical Research Letters*, 39(1), n/a–n/a. <https://doi.org/10.1029/2011GL050197>
- 549 Chow, V. T. (1959). *Open-channel hydraulics*.
- 550 CPRA. (2017). *Louisiana's Comprehensive Master Plan for a Sustainable Coast*. Baton Rouge, LA: State of
551 Louisiana. Retrieved from <http://coastal.la.gov/our-plan/>
- 552 Edmonds, D. A. (2012). Stability of backwater-influenced river bifurcations: A study of the Mississippi-Atchafalaya
553 system. *Geophysical Research Letters*, 39(8), n/a–n/a. <https://doi.org/10.1029/2012GL051125>
- 554 Engelund, F., & Hansen, E. (1967). *A Monograph on Sediment Transport in Alluvial Streams*. Copenhagen: Teknik
555 Forlag.
- 556 Fisk, H. N. (1952). *Geological investigation of the Atchafalaya Basin and the problem of Mississippi River*
557 *diversion*. Vicksburg, Mississippi: U.S. Corps of Engineers, Mississippi River Commission.

- 558 Galler, J. J., Bianchi, T. S., Alison, M. A., Wysocki, L. A., Campanella, R., Narasimhan, T. N., et al. (2003).
559 Biogeochemical implications of levee confinement in the lowermost Mississippi River. *EOS [American*
560 *Geophysical Union Transactions]*, 84(44), 469–484.
- 561 Ganti, V., Chu, Z., Lamb, M. P., Nittrouer, J. A., & Parker, G. (2014). Testing morphodynamic controls on the
562 location and frequency of river avulsions on fans versus deltas: Huanghe (Yellow River), China.
563 *Geophysical Research Letters*, 41(22), 2014GL061918. <https://doi.org/10.1002/2014GL061918>
- 564 Ganti, V., Chadwick, A. J., Hassenruck-Gudipati, H. J., & Lamb, M. P. (2016). Avulsion cycles and their
565 stratigraphic signature on an experimental backwater-controlled delta. *Journal of Geophysical Research:*
566 *Earth Surface*, 121(9), 1651–1675. <https://doi.org/10.1002/2016JF003915>
- 567 Ganti, V., Chadwick, A. J., Hassenruck-Gudipati, H. J., Fuller, B. M., & Lamb, M. P. (2016). Experimental river
568 delta size set by multiple floods and backwater hydrodynamics. *Science Advances*, 2(5), e1501768.
569 <https://doi.org/10.1126/sciadv.1501768>
- 570 Gasparini, N., & Yuill, B. T. (2020). High Water: Prolonged Flooding on the Deltaic Mississippi River. Retrieved
571 May 19, 2020, from <https://eos.org/features/high-water-prolonged-flooding-on-the-deltaic-mississippi-river>
- 572 Hajek, E. A., & Edmonds, D. A. (2014). Is river avulsion style controlled by floodplain morphodynamics? *Geology*,
573 42(3), 199–202. <https://doi.org/10.1130/G35045.1>
- 574 Hoitink, A. J. F., Nittrouer, J. A., Passalacqua, P., Shaw, J. B., Langendoen, E. J., Huisman, Y., & Maren, D. S.
575 van. (2020). Resilience of river deltas in the Anthropocene. *Journal of Geophysical Research: Earth*
576 *Surface*, e2019JF005201. <https://doi.org/10.1029/2019JF005201>
- 577 Jerolmack, D. J., & Swenson, J. B. (2007). Scaling relationships and evolution of distributary networks on wave-
578 influenced deltas. *Geophysical Research Letters*, 34(23), L23402. <https://doi.org/10.1029/2007GL031823>
- 579 Kafadar, K. (2014). Notched Box-And-Whisker Plot. In *Wiley StatsRef: Statistics Reference Online*. American
580 Cancer Society. <https://doi.org/10.1002/9781118445112.stat00467>
- 581 Karim, F. (1995). Bed Configuration and Hydraulic Resistance in Alluvial-Channel Flows. *Journal of Hydraulic*
582 *Engineering*, 121(1), 15–25. [https://doi.org/10.1061/\(ASCE\)0733-9429\(1995\)121:1\(15\)](https://doi.org/10.1061/(ASCE)0733-9429(1995)121:1(15))
- 583 Kenney, M. A., Hobbs, B. F., Mohrig, D., Huang, H., Nittrouer, J. A., Kim, W., & Parker, G. (2013). Cost analysis
584 of water and sediment diversions to optimize land building in the Mississippi river delta. *Water Resources*
585 *Research*. <https://doi.org/10.1002/wrcr.20139>

- 586 Kesel, R. H. (2003). Human modifications to the sediment regime of the Lower Mississippi River flood plain.
587 *Geomorphology*, 56(3), 325–334. [https://doi.org/10.1016/S0169-555X\(03\)00159-4](https://doi.org/10.1016/S0169-555X(03)00159-4)
- 588 Kleinhans, M. G., Cohen, K. M., Hoekstra, J., & IJmker, J. M. (2011). Evolution of a bifurcation in a meandering
589 river with adjustable channel widths, Rhine delta apex. *Earth Surface Processes and Landforms*, 36(15),
590 2011–2027. <https://doi.org/10.1002/esp.2222>
- 591 Kleinhans, M. G., Ferguson, R. I., Lane, S. N., & Hardy, R. J. (2012). Splitting rivers at their seams: bifurcations
592 and avulsion. *Earth Surface Processes and Landforms*. <https://doi.org/10.1002/esp.3268>
- 593 Knox, R. L., & Latrubesse, E. M. (2016). A geomorphic approach to the analysis of bedload and bed morphology of
594 the Lower Mississippi River near the Old River Control Structure. *Geomorphology*, 268, 35–47.
595 <https://doi.org/10.1016/j.geomorph.2016.05.034>
- 596 Lamb, M. P., Nittrouer, J. A., Mohrig, D., & Shaw, J. B. (2012). Backwater and river plume controls on scour
597 upstream of river mouths: Implications for fluvio-deltaic morphodynamics. *Journal of Geophysical*
598 *Research*, 117(F1), F01002. <https://doi.org/10.1029/2011JF002079>
- 599 Lane, E. W. (1957). *A Study of the Shape of Channels Formed by Natural Streams Flowing in Erodible Material*
600 (Missouri River Division Sediment Series Report 9) (pp. 1–106). Omaha, Nebraska: U.S. Army Corps of
601 Engineers.
- 602 Latimer, R. A., & Schweitzer, C. W. (1951). *The Atchafalaya River study: A report based engineering and*
603 *geological studies of the enlargement of Old and Atchafalaya Rivers* (Vol. 1,2,3). Vicksburg, Mississippi:
604 U.S. Army Corps of Engineers, Mississippi River Commission.
- 605 Lazarus, E. D., & Goldstein, E. B. (2019). Is There a Bulldozer in your Model? *Journal of Geophysical Research:*
606 *Earth Surface*, 124(3), 696–699. <https://doi.org/10.1029/2018JF004957>
- 607 Martin, J., Sheets, B., Paola, C., & Hoyal, D. (2009). Influence of steady base-level rise on channel mobility,
608 shoreline migration, and scaling properties of a cohesive experimental delta. *Journal of Geophysical*
609 *Research: Earth Surface*, 114(F3). <https://doi.org/10.1029/2008JF001142>
- 610 McCain, G. (2016). Influences of Channel Dredging on Avulsion Potential at the Atchafalaya River. *Theses and*
611 *Dissertations*. Retrieved from <https://scholarworks.uark.edu/etd/1559>
- 612 McPhee, J. (1987, February 16). Atchafalaya. Retrieved from
613 <https://www.newyorker.com/magazine/1987/02/23/atchafalaya>

- 614 Mohrig, D., Heller, P. L., Paola, C., & Lyons, W. J. (2000). Interpreting avulsion process from ancient alluvial
615 sequences: Guadalupe-Matarranya system (northern Spain) and Wasatch Formation (western Colorado).
616 *Geological Society of America Bulletin*, *112*(12), 1787–1803.
- 617 Mossa, J. (2013). Historical changes of a major juncture: Lower Old River, Louisiana. *Physical Geography*, *34*(4–
618 05), 315–334. <https://doi.org/10.1080/02723646.2013.847314>
- 619 Mossa, J. (2016). The changing geomorphology of the Atchafalaya River, Louisiana: A historical perspective.
620 *Geomorphology*, *252*, 112–127. <https://doi.org/10.1016/j.geomorph.2015.08.018>
- 621 Nittrouer, J. A., Shaw, J. B., Lamb, M. P., & Mohrig, D. (2012). Spatial and temporal trends for water-flow velocity
622 and bed-material transport in the lower Mississippi River. *Geol. Soc. Am. Bull.*, *124*, 400–414.
623 <https://doi.org/10.1130/B30497.1>
- 624 Parker, G. (2004). *1D Sediment Transport Morphodynamics with applications to Rivers and Turbidity Currents*.
625 Retrieved from [http://hydrolab.illinois.edu/people/parkerg/morphodynamics_e-](http://hydrolab.illinois.edu/people/parkerg/morphodynamics_e-book.htm?q=people/parkerg/morphodynamics_e-book.htm)
626 [book.htm?q=people/parkerg/morphodynamics_e-book.htm](http://hydrolab.illinois.edu/people/parkerg/morphodynamics_e-book.htm)
- 627 Peyronnin, N. S., Caffey, R. H., Cowan, J. H., Justic, D., Kolker, A. S., Laska, S. B., et al. (2017). Optimizing
628 Sediment Diversion Operations: Working Group Recommendations for Integrating Complex Ecological
629 and Social Landscape Interactions. *Water*, *9*(6), 368. <https://doi.org/10.3390/w9060368>
- 630 Ribberink, J. S., & Van Der Sande, J. T. M. (1985). Aggradation in rivers due to overloading - analytical
631 approaches. *Journal of Hydraulic Research*, *23*(3), 273–283. <https://doi.org/10.1080/00221688509499355>
- 632 Roberts, H., Adams, R., & Cunningham, R. (1980). Evolution of sand-dominant subaerial phase, Atchafalaya Delta,
633 Louisiana. *American Association of Petroleum Geologists Bulletin*, *64*, 264–279.
- 634 Saucier, R. T. (1994). *Geomorphology and Quarternary Geologic History of the Lower Mississippi Valley. Volume*
635 *2*. DTIC Document. Retrieved from
636 <http://oai.dtic.mil/oai/oai?verb=getRecord&metadataPrefix=html&identifier=ADA299155>
- 637 Shanno, D. F. (1970). Conditioning of quasi-Newton methods for function minimization. *Mathematics of*
638 *Computation*, *24*(111), 647–656.
- 639 Shaw, J. B., & McElroy, B. (2016). Backwater number scaling of alluvial bed forms. *Journal of Geophysical*
640 *Research: Earth Surface*, *121*(8), 2016JF003861. <https://doi.org/10.1002/2016JF003861>

- 641 Shaw, J. B., Estep, J. D., Whaling, A. R., Sanks, K. M., & Edmonds, D. A. (2018). Measuring subaqueous
642 progradation of the Wax Lake Delta with a model of flow direction divergence. *Earth Surface Dynamics*,
643 6(4), 1155–1168. <https://doi.org/10.5194/esurf-6-1155-2018>
- 644 Slingerland, R., & Smith, N. D. (2004). River avulsions and their deposits. *Annu. Rev. Earth Planet. Sci.*, 32, 257–
645 285.
- 646 Smith, L. M., & Winkley, B. R. (1996). The response of the Lower Mississippi River to river engineering.
647 *Engineering Geology*, 45(1), 433–455. [https://doi.org/10.1016/S0013-7952\(96\)00025-7](https://doi.org/10.1016/S0013-7952(96)00025-7)
- 648 Syvitski, J. P. M. (2008). Deltas at risk. *Sustainability Science*, 3(1), 23–32. <https://doi.org/10.1007/s11625-008->
649 0043-3
- 650 Tessler, Z. D., Vörösmarty, C. J., Grossberg, M., Gladkova, I., Aizenman, H., Syvitski, J. P. M., & Foufoula-
651 Georgiou, E. (2015). Profiling risk and sustainability in coastal deltas of the world. *Science*, 349(6248),
652 638–643. <https://doi.org/10.1126/science.aab3574>
- 653 Törnqvist, T. E., & Bridge, J. S. (2002). Spatial variation of overbank aggradation rate and its influence on avulsion
654 frequency. *Sedimentology*, 49(5), 891–905.
- 655 Tye, R. S., & Coleman, J. M. (1989). Evolution of Atchafalaya lacustrine deltas, south-central Louisiana.
656 *Sedimentary Geology*, 65(1), 95–112. [https://doi.org/10.1016/0037-0738\(89\)90008-0](https://doi.org/10.1016/0037-0738(89)90008-0)
- 657 USACE. (1915). *1913 Mississippi River Hydrographic Survey*. Retrieved from
658 <https://www.mvn.usace.army.mil/Missions/Engineering/Geospatial->
659 [Section/MRHB_Historic/MRHB_1913/](https://www.mvn.usace.army.mil/Missions/Engineering/Geospatial-Section/MRHB_Historic/MRHB_1913/)
- 660 USACE. (1950). *1949 Mississippi River Hydrographic Survey*. Retrieved from
661 <https://www.mvn.usace.army.mil/Missions/Engineering/Geospatial->
662 [Section/MRHB_Historic/MRHB_1913/](https://www.mvn.usace.army.mil/Missions/Engineering/Geospatial-Section/MRHB_Historic/MRHB_1913/)
- 663 USACE. (2009). Old River Control. U.S. Army Corps of Engineers, New Orleans District. Retrieved from
664 <https://www.mvn.usace.army.mil/Portals/56/docs/PAO/Brochures/OldRiverControlBrochure.pdf>
- 665 Vinh, V. D., Ouillon, S., Thanh, T. D., & Chu, L. V. (2014). Impact of the Hoa Binh dam (Vietnam) on water and
666 sediment budgets in the Red River basin and delta. *Hydrology and Earth System Sciences*, 18(10), 3987–
667 4005. <https://doi.org/10.5194/hess-18-3987-2014>

- 668 Viparelli, E., Nittrouer, J. A., & Parker, G. (2015). Modeling flow and sediment transport dynamics in the
669 lowermost Mississippi River, Louisiana, USA, with an upstream alluvial-bedrock transition and a
670 downstream bedrock-alluvial transition: Implications for land building using engineered diversions.
671 *Journal of Geophysical Research: Earth Surface*, 120(3), 534–563. <https://doi.org/10.1002/2014JF003257>
- 672 Wang, B., & Xu, Y. J. (2016). Long-term geomorphic response to flow regulation in a 10-km reach downstream of
673 the Mississippi–Atchafalaya River diversion. *Journal of Hydrology: Regional Studies*, 8, 10–25.
674 <https://doi.org/10.1016/j.ejrh.2016.08.002>
- 675 Wang, B., & Xu, Y. J. (2018). Decadal-Scale Riverbed Deformation and Sand Budget of the Last 500 km of the
676 Mississippi River: Insights Into Natural and River Engineering Effects on a Large Alluvial River. *Journal*
677 *of Geophysical Research: Earth Surface*, 123(5), 874–890. <https://doi.org/10.1029/2017JF004542>
- 678 Wang, Z. B., De Vries, M., Fokkink, R. J., & Langerak, A. (1995). Stability of river bifurcations in ID
679 morphodynamic models. *Journal of Hydraulic Research*, 33(6), 739–750.
- 680 Wilson, C., Goodbred, S., Small, C., Gilligan, J., Sams, S., Mallick, B., & Hale, R. (2017). Widespread infilling of
681 tidal channels and navigable waterways in human-modified tidal delta plain of southwest Bangladesh. *Elem-*
682 *Sci Anth*, 5(0). <https://doi.org/10.1525/elementa.263>
- 683 Wu, C.-Y., & Mossa, J. (2019). Decadal-Scale Variations of Thalweg Morphology and Riffle–Pool Sequences in
684 Response to Flow Regulation in the Lowermost Mississippi River. *Water*, 11(6), 1175.
685 <https://doi.org/10.3390/w11061175>
- 686 Ying, X., & Wang, S. S. Y. W. (2008). Improved implementation of the HLL approximate Riemann solver for one-
687 dimensional open channel flows. *Journal of Hydraulic Research*, 46(1), 21–34.
688 <https://doi.org/10.1080/00221686.2008.9521840>
- 689 Ying, X., Khan Abdul A., & Wang Sam S. Y. (2004). Upwind Conservative Scheme for the Saint Venant Equations.
690 *Journal of Hydraulic Engineering*, 130(10), 977–987. [https://doi.org/10.1061/\(ASCE\)0733-](https://doi.org/10.1061/(ASCE)0733-9429(2004)130:10(977))
691 [9429\(2004\)130:10\(977\)](https://doi.org/10.1061/(ASCE)0733-9429(2004)130:10(977))

692

693

694